BJA

British Journal of Anaesthesia, 125 (1): 55–66 (2020)

doi: 10.1016/j.bja.2020.02.027
Advance Access Publication Date: 1 June 2020
Neuroscience and Neuroanaesthesia

NEUROSCIENCE AND NEUROANAESTHESIA

Cohort study into the neural correlates of postoperative delirium: the role of connectivity and slow-wave activity

Sean Tanabe[1], Rosaleena Mohanty[1,2], Heidi Lindroth[1,3], Cameron Casey[1], Tyler Ballweg[1], Zahra Farahbakhsh[1], Bryan Krause[1], Vivek Prabhakaran[2], Matthew I. Banks[1] and Robert D. Sanders[1,4,5,*]

[1]Department of Anesthesiology, University of Wisconsin, Madison, WI, USA, [2]Department of Radiology, University of Wisconsin, Madison, WI, USA, [3]Center for Health Innovation and Implementation Science, Center for Aging Research, Division of Pulmonary and Critical Care Medicine, Regenstrief Institute, Indiana University School of Medicine, Indianapolis, IN, USA, [4]University of Sydney, Australia and [5]Department of Anaesthetics, Royal Prince Alfred Hospital, Australia

*Corresponding author. E-mail: robert.sanders@sydney.edu.au

Abstract

Background: Delirium frequently affects older patients, increasing morbidity and mortality; however, the pathogenesis is poorly understood. Herein, we tested the cognitive disintegration model, which proposes that a breakdown in fronto-parietal connectivity, provoked by increased slow-wave activity (SWA), causes delirium.
Methods: We recruited 70 surgical patients to have preoperative and postoperative cognitive testing, EEG, blood biomarkers, and preoperative MRI. To provide evidence for causality, any putative mechanism had to differentiate on the diagnosis of delirium; change proportionally to delirium severity; and correlate with a known precipitant for delirium, inflammation. Analyses were adjusted for multiple corrections (MCs) where appropriate.
Results: In the preoperative period, subjects who subsequently incurred postoperative delirium had higher alpha power, increased alpha band connectivity (MC $P<0.05$), but impaired structural connectivity (increased radial diffusivity; MC $P<0.05$) on diffusion tensor imaging. These connectivity effects were correlated ($r^2=0.491$; $P=0.0012$). Postoperatively, local SWA over frontal cortex was insufficient to cause delirium. Rather, delirium was associated with increased SWA involving occipitoparietal and frontal cortex, with an accompanying breakdown in functional connectivity. Changes in connectivity correlated with SWA ($r^2=0.257$; $P<0.0001$), delirium severity rating ($r^2=0.195$; $P<0.001$), interleukin 10 ($r^2=0.152$; $P=0.008$), and monocyte chemoattractant protein 1 ($r^2=0.253$; $P<0.001$).
Conclusions: Whilst frontal SWA occurs in all postoperative patients, delirium results when SWA progresses to involve posterior brain regions, with an associated reduction in connectivity in most subjects. Modifying SWA and connectivity may offer a novel therapeutic approach for delirium.
Clinical trial registration: NCT03124303, NCT02926417

Keywords: cognitive dysfunction; connectivity; delirium; electroencephalogram; inflammation; mechanism; postoperative; slow wave activity; surgery

Received: 4 November 2019; **Accepted:** 28 February 2020

Editor's key points

- Electroencephalographic slow-wave activity has previously been associated with delirium.
- We found local SWA in patients without delirium but global SWA in patients with delirium.
- A distinguishing feature of postoperative delirium in most patients was a decrease in correlates of frontoparietal connectivity.
- Decreased preoperative structural rather than functional connectivity was predictive of postoperative delirium.

Delirium is a sudden onset of confusion that frequently affects older patients.[1] It is associated with increased morbidity, mortality, loss of functional independence, and worsening quality of life, and may herald the onset of cognitive decline and dementia.[1,2] It is estimated to cost $160 billion per annum in the USA.[3] The pathogenesis of delirium remains obscure; whilst several theories have been proposed,[4–7] no therapies have been forthcoming. We proposed a cognitive disintegration model,[7] whereby the severe cognitive symptoms of delirium are related to breakdown in connectivity driven by increased EEG slow-wave activity (SWA) in key frontoparietal cognitive networks. Inspired by the basic tenets of cognitive frameworks, such as integrated information theory[8] and predictive coding,[9] we surmised that cognition requires the *integration of information* from functionally specialised brain regions to form a coherent view of self and the environment. Delirium is characterised by fragmented perceptions and disjointed interactions with the environment, consistent with disintegration of certain cognitive processes. Preliminary evidence for this model, based on reductions in connectivity during delirium, has been provided by Numan and colleagues[10] and van Dellen and colleagues.[11] However, the case-control design used does not exclude premorbid differences between the groups. We hypothesised that pre-existing decreases in connectivity would predispose to delirium.[7] Thus, we collected EEG data preoperatively, before delirium occurred. The electrophysiological hallmark of delirium is cortical SWA. Cortical SWA is a characteristic of both deep non-rapid eye movement sleep[12] and anaesthesia.[13] In both of these states, it is associated with reduced connectivity. Hence, it is plausible that delirium-associated SWA may lead to impairments in connectivity.

As there is presently no way of reversing delirium to establish causality, we used the Bradford Hill criteria for causation to support the importance of the mechanisms uncovered. Hence, we sought a *strong* association, with *specific* changes in the delirious population that changed *contemporaneously* with delirium and with a *biological gradient*. To achieve these criteria, the change with transition to delirium must differ from non-delirious subjects *and* should also change proportionately to delirium symptom severity (henceforth, delirium severity). These criteria also impose a relatively stringent statistical threshold: requiring a test to be significant for both delirium incidence and severity would exclude spurious results at a threshold equivalent to 0.05^2. Furthermore, to provide *biological plausibility*, we hypothesised that relevant effects should also correlate with inflammation, a probable precipitant of delirium. To identify relevant markers of systemic inflammation, we identified plasma cytokines that changed with both delirium incidence and severity.

Whilst multiple studies have shown that delirium is associated with diffuse slowing in the EEG,[14] they typically have not accounted for pre-delirium status or within- and across-subject differences. Nor have they looked for Bradford Hill criteria of causation nor related findings to severity or inflammation. Herein, we took advantage of major elective surgery, where the precipitating event for delirium is predictable in time. We tested our hypothesis that, when SWA progressed to involve frontoparietal brain regions, the associated breakdown in connectivity would precipitate delirium.[7]

Methods

The data are derived from two ongoing perioperative cohort studies registered with https://clinicaltrials.gov/(Interventions for Postoperative Delirium: Biomarker-3 (IPOD-B3), NCT03124303, and Interventions for Postoperative Delirium: Biomarker-2 (IPOD-B2), NCT02926417) and approved by the University of Wisconsin–Madison Institutional Review Board (#2015-0374; 2015-0960). EEG data were collected from 72 patients before and after surgery between 2015 and 2019. Two subjects' data were excluded because of poor impedance contaminating the entire recording. After exclusion of these two subjects, all available EEG data (in subjects with paired preoperative and postoperative EEG) collected until 70 subjects were recruited were used in the analyses (Fig. 1). Eight subjects were recruited only to IPOD-B2 and 62 to IPOD-B3. Sensitivity analyses, conducted only on subjects recruited to IPOD-B3, found similar results. IPOD-B2 is a small ongoing cohort study of adult subjects undergoing thoracic aortic aneurysm repair (open or endovascular; Supplementary Table 1). IPOD-B3 is a larger ongoing cohort of adult patients (>65 yr old) undergoing major surgery (Supplementary Table 1).

Cohort sample size

A priori power analysis suggested that a minimum of 59 subjects would be required to show EEG differences in delirium. Prior data suggested an effect size for a 'between-subject' analysis of a three-fold increase in SWA[11] in delirium. Based on the variance in SWA from van Dellen and colleagues,[11] power analysis suggests that 12 delirious subjects, compared with 47 controls, will provide 99% power for an uncorrected $\alpha<0.001$ to detect SWA differences assuming a 20% delirium incidence. Calculation of SWA differences required paired EEG samples for preoperative and postoperative data from which we could calculate the change in the delirious subjects and compare with the change in the non-delirious subjects.

Delirium diagnosis

The 70 subjects were grouped depending on postoperative confusion assessment method diagnoses of delirium (confusion assessment method [CAM]+/–[15,16] or CAM-ICU+/– if ventilated[17]) status at the time of the EEG recording as delirious or not.[15] The delirium group contained 22 subjects and the non-delirium group contained 48 subjects. Delirium severity was scored using the Delirium Rating of Severity-98 (DRS).[18] Weekly delirium review meetings were held to ensure consistency of scoring during the data collection period.

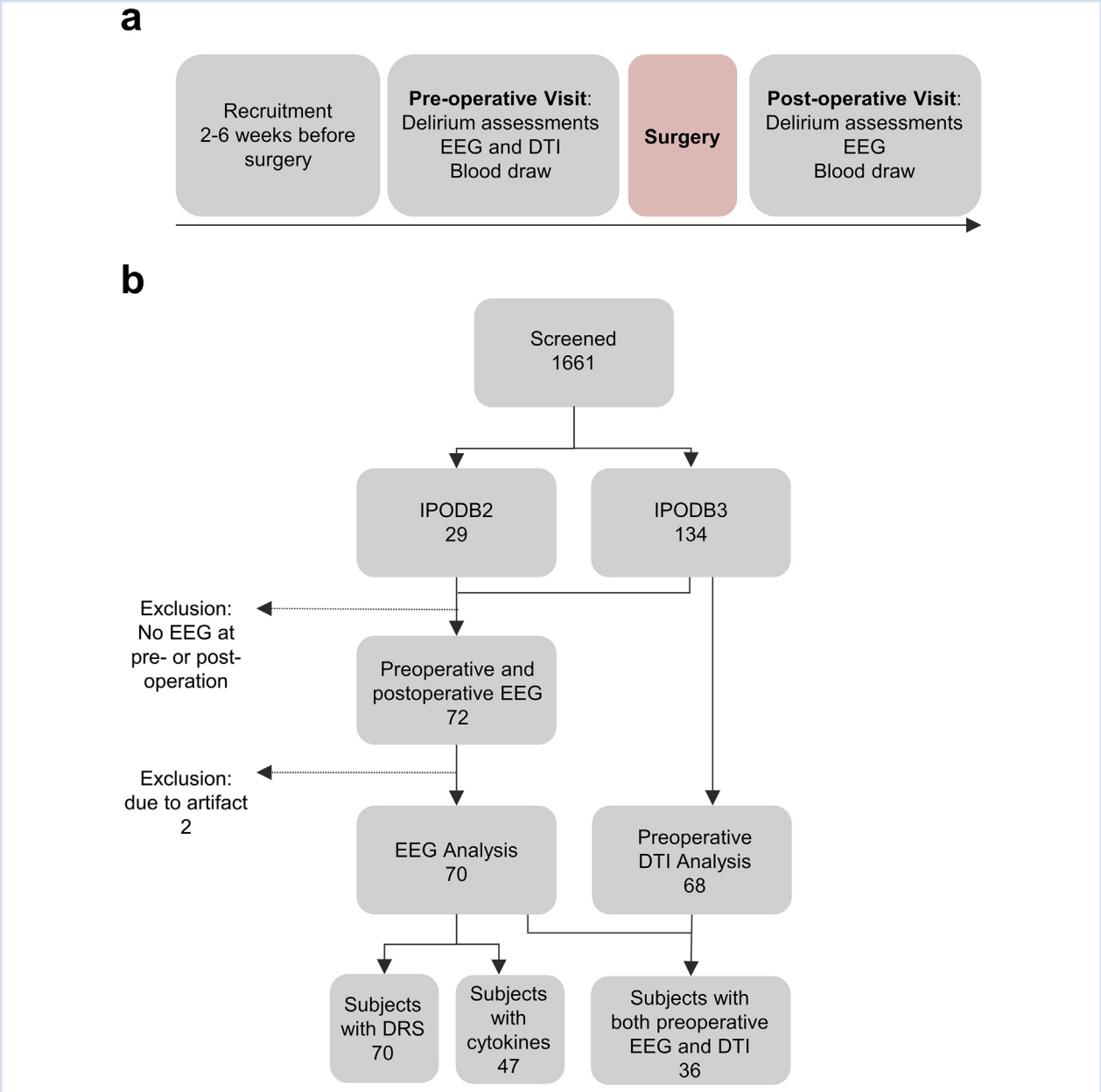

Fig 1. Study design and Strengthening the Reporting of Observational Studies in Epidemiology (STROBE) diagram. (a) Study design. Delirium severity (DRS) is collected during both preoperative and postoperative delirium assessment. (b) STROBE diagram. Data are from IPOD-B2 and IPOD-B3 ongoing perioperative cohort studies. DRS, Delirium Rating of Severity-98; DTI, diffusion tensor imaging; IPOD-B2, Interventions for Postoperative Delirium: Biomarker-2; IPOD-B3, Interventions for Postoperative Delirium: Biomarker-3.

EEG recording and preprocessing

EEG data were collected using high-density EEG with 256 channels (Electrical Geodesics, Inc., Eugene, OR, USA) using a sampling frequency of 250 Hz (five subjects were recorded at 500 Hz; these were down sampled to 250 Hz). Data were collected preoperatively with a median of 5 days before surgery (inter-quartile range [IQR]: 1–7 days) and postoperatively with a median of the first postoperative day (IQR: 1–1 day). For each subject and condition, 15 min of eyes-closed resting-state data were collected. In three subjects, eyes-open data for a minimum of 90 s were collected allowing comparison of eyes open and closed.

These data were filtered from 0.1 to 50 Hz using Hamming windowed-sinc FIR filter. Channels and data segments containing artifact were visually inspected and removed. To remove artifact of eye movement and muscle movement, we applied independent component analysis in EEGLAB. Before analysis, the removed channels were interpolated, and then the signals were average-referenced.

Spectral power

The data were estimated for power spectral density with Welch's method into delta (0.5–4 Hz), theta (4–6 Hz), alpha (6–12 Hz), beta (12–28 Hz), and gamma (28–40 Hz). The power spectral density was log10 transformed to normalise the distribution. Slow-wave activity was *post hoc* defined as 0.5–6 Hz similar to prior definitions.[19]

Phase lag index

To measure the functional connectivity between channel signals, the debiased weighted phase lag index (PLI) in the FieldTrip toolbox (maintained by the Donders Institute for Brain, Cognition, and Behaviour which is part of Radboud University in Nijmegen, the Netherlands) was used.[20] Phase lag index alone estimates the degree to which the two time-series leads and lags by indexing their phase differences. However, PLI is sensitive to signal synchronisations because of volume conduction. By weighting the phases across cross-spectrum time series, PLI is able to mitigate the sensitivity to volume conduction.[20] Debiased weighted PLI further estimates the squared weighted PLI to normalise the positive bias.

Between all 256 channels, in a pairwise manner, we calculate debiased PLI using 2 s window length and 25% overlap. To probe changes associated with detectable SWA in both the delirious and non-delirious groups, we divided the 256 scalp electrodes in 25 squares (Supplementary Fig. 1). The PLI between these 'squares' were averaged, producing pairwise-squared PLI. We focused on PLI involving the midline frontal square centred on the Fz electrode, which showed increased SWA in both delirious and non-delirious subjects. However, we also conducted pairwise analyses across connections and correlated these changes in connectivity with delirium severity. These analyses were corrected by false discovery rate (FDR) methods. We also plot a PLI spectrum by using the cross-spectra produced from multi-taper frequency transformation (see Supplementary data for methods).

EEG statistical analysis

To test for topographical differences or correlations, two-tailed statistical non-parametric mapping (SNPM) threshold-free cluster enhancement was used.[21] Wilcoxon rank-sum test, Wilcoxon signed-rank test, and Pearson correlation were used for non-topographical tests where appropriate. To test for differences amongst groups (across delirium status and pre-/postoperation), we used linear mixed-effects models, testing the interaction of delirium status and time point (pre *vs* post) for each frequency band. Test statistics and *P*-values were calculated using Type III Wald *F*-tests with Kenward–Roger degrees of freedom.

Topographical PLI analyses use parametric Pearson correlation on each PLI connection. These analyses are sensitive to outlier influence, as parametric tests assume a homogeneous variance. Therefore, for each PLI connectivity, we excluded outlier subjects whose Cook's distance is above 4*(mean of Cook's distance).[22] Excluding subjects with large Cook's distances resulted in substantial changes to the regression model estimation. As each PLI connectivity topoplot has a different regression model, there will be a different number of subjects excluded for each connection. Because of this, analyses making use of Cook's distance will indicate sample size as a range (e.g. n=70 [64–69, after outlier exclusion]). The PLI analyses were corrected by FDR methods.

Blood biomarkers

We also collected blood samples for biomarker analyses immediately before and after the resting-state EEG. Plasma samples were collected in ethylenediamine tetra-acetic acid (EDTA)-containing tubes preoperatively and stored at −80°C.

Cytokine analysis

A multiplex assay was conducted at Eve Technologies (Montreal, Canada) for plasma samples that were paired with EEG collection. The cytokines measured were interleukin (IL) 1 (IL-1) beta, IL-1 receptor antagonist, IL-2, IL-4, IL-6, IL-8, IL-10, IL-12, monocyte chemoattractant protein 1 (MCP-1), and tumour necrosis factor-alpha. For the cytokine analysis only, subjects were excluded if they had no blood drawn around the time of the EEG recording.

Diffusion tensor imaging methods

A *post hoc* decision was made during the analysis of EEG data to investigate preoperative structural connectivity (diffusion tensor imaging [DTI]) in patients with EEG to investigate an unexpected finding with preoperative frontal EEG connectivity. All available DTI data in the cohort are reported. Of the patients recruited to IPOD-B3, 75 patients consented to preoperative imaging (there is no imaging collected in IPOD-B2). Six of the DTI scans were discarded because of motion artifact. Preoperative DTI scans were available from 68 patients (17 delirious) after quality control and preprocessing. Thirty-six subjects had preoperative imaging and EEG. MRI data were collected on 3.0 T whole-body scanner (General Electric Medical Systems, Waukesha, WI, USA) with an eight-channel head coil. Diffusion tensor imaging data were acquired with the following diffusion parameters: single-shot echo planar imaging, repetition time=9000 ms, echo time=66.2 ms, single average (NEX) 1, field of view 256×256 mm^2, voxel size 1×1×2 mm^3, 75 axial slices with no gap between slices, flip angle 90°, 56 gradient encoded directions, and b-values of 0 and 1000 s mm^{-2}.

The raw DTI were checked manually for quality control, and each remaining scan was corrected for head motion and eddy-current distortion with the *eddy*[23] tool and skull stripping and removal of non-tissue components in FSL.[24] The diffusion tensor model, based on the least-squares fit, was applied using FDT's *dtifit* providing data on fractional anisotropy (FA), mean diffusivity (MD), axial diffusivity (AD), and radial diffusivity (RD). Non-linear registration was conducted using Advanced Normalization Tools (ANTs is maintained by the Penn Image Computing and Science Lab which is operated out of the University of Pennsylvania in Philadelphia, PA, USA)[25] to a standard template based on the publicly available Mayo Clinic Adult Lifespan Template atlas.[26]

Prior data emphasised RD,[27] and hence, we pursued that as our primary DTI metric, although convergent results were obtained with MD. Voxel-wise skeletonised white matter tract maps were obtained for each DTI metric with tract-based spatial statistics (TBSS),[28] applied to AD, MD, and RD, and were used to perform cross-subject statistical analyses. Voxel-wise statistical approach (*randomise* tool[21] with threshold-free cluster enhancement) was adopted to study the association between the preprocessed and TBSS-based white matter

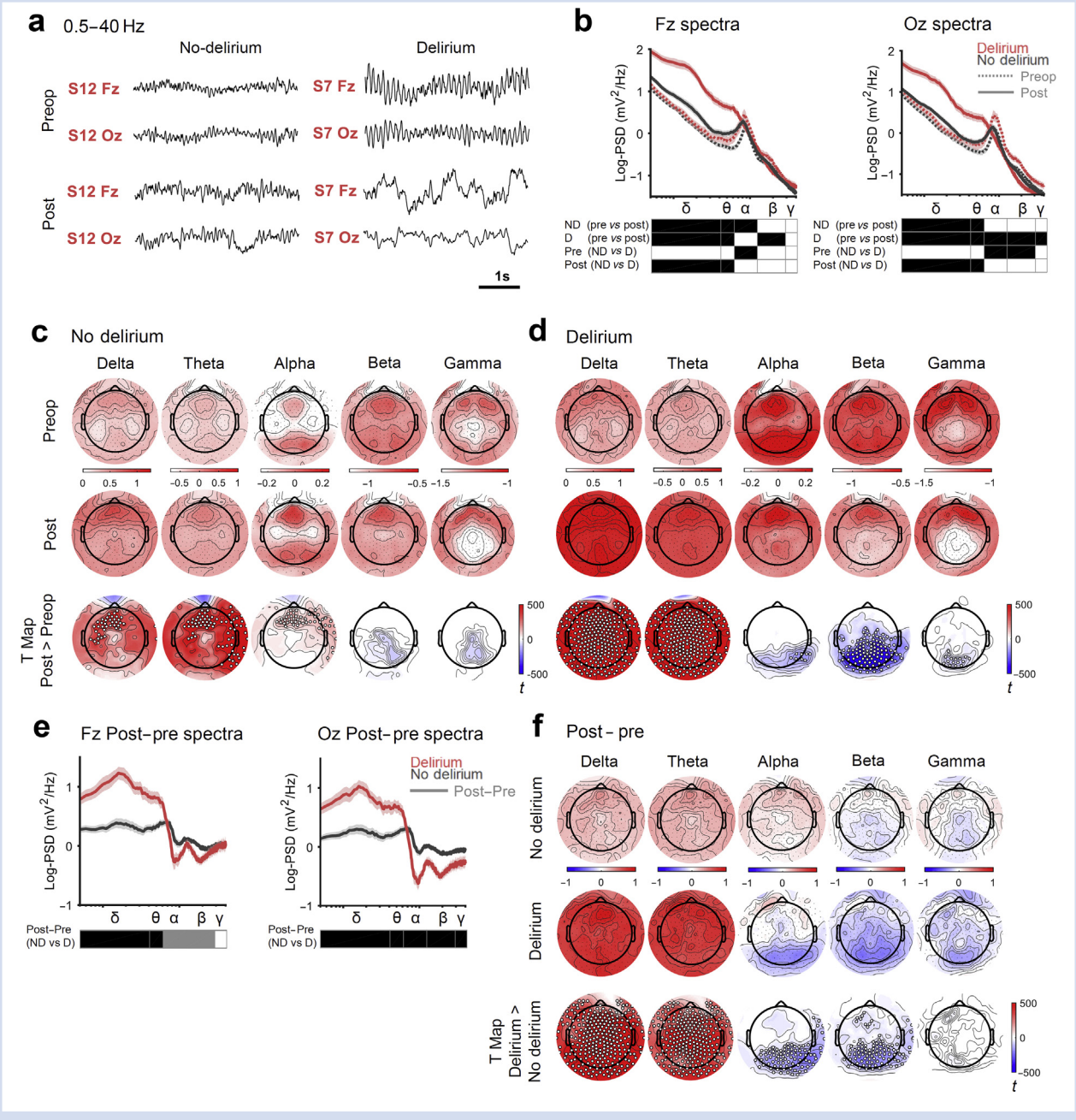

Fig 2. Delirium occurs with increased global slow-wave activity and loss of posterior high-frequency activity. (a) Representative EEG signals from two electrodes, one frontal (Fz) and one posterior/occipital (Oz), collected preoperatively (Preop/Pre) and postoperatively (Post). (b) Group-level spectral analysis comparing patients preoperatively and postoperatively for patients who do (D), or do not (ND), incur delirium ($P<0.05$ [black squares], linear mixed-effects model across delirium status and operative phase). Spectra range from 0.5 to 40 Hz, statistics were completed for frequency bands; δ 0.5–4 Hz, θ 4–6 Hz, α 6–12 Hz, β 12–28 Hz, γ 28–40 Hz. The alpha band range (α), 6–12 Hz, was chosen by inspecting the peak in the mean spectra amongst all subjects. Topological spectral power of the preoperative and postoperative states for patients who do not incur delirium (c) or do incur delirium (d) across each power band. The third row shows the post-operative>preoperative contrast *t*-maps, corrected with threshold-free cluster enhancement (TFCE), with overlaid electrodes showing significant differences (statistical non-parametric mapping [SNPM] paired; corrected TFCE $P<0.05$ [white dots]). (e) Spectral analysis for the transition in state (postoperatively-preoperatively) for subjects who incur delirium or do not ($P<0.05$ [black squares] after FDR correction with two-sided rank-sum test) for electrodes Fz and Oz. Grey square: uncorrected $P<0.05$. (f) Topological contrasts of the transition to the non-delirious *vs* delirious state (first two rows). Third row shows the TFCE *t*-map of two groups contrast with significant electrodes overlaid (SNPM unpaired; TFCE corrected $P<0.05$ *t*-map). For all statistics, $n_{ND}=48$ and $n_{D}=22$. PSD, power spectral density.

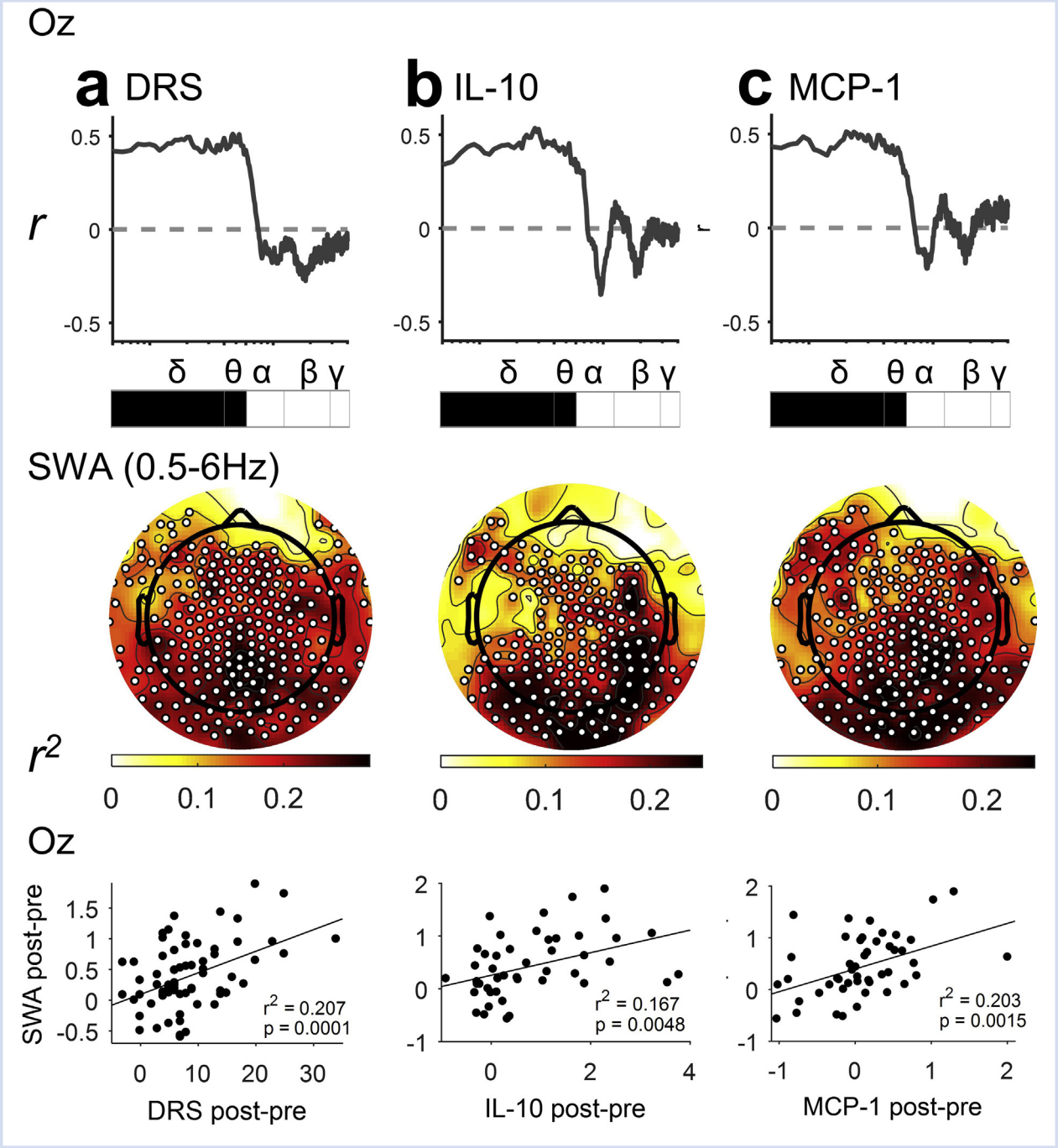

Fig 3. Posterior slow-wave activity (SWA) is associated with (a) delirium severity and (b, c) systemic inflammation. Each column represents the correlation of change in power (postoperatively-preoperatively) with an outcome either Delirium Rating of Severity-98 (DRS), interleukin (IL)-10, or monocyte chemoattractant protein 1 (MCP-1). Top row shows correlation with transition in spectral power across frequencies from occipital electrode (Oz). Spectra range from 0.5 to 40 Hz; statistics done on frequency bands; δ 0.5–4 Hz, θ 4–6 Hz, α 6–12 Hz, β 12–28 Hz, and γ 28–40 Hz. Black square: $P<0.05$ after false discovery rate correction. Grey square: $P<0.05$ uncorrected. Middle row shows topological correlation with the increase in SWA (0.5–6 Hz; statistical non-parametric mapping correlation; corrected threshold-free cluster enhancement $P<0.05$ [white dots show statistically significant electrodes]). Bottom row shows correlation with transition in SWA from occipital electrode Oz. DRS $n=70$; IL-8 $n=47$; IL-10 $n=46$; MCP-1 $n=47$.

skeletonised maps and delirium incidence, and severity on a group level (using 10 000 permutations). Voxel-wise statistical significance inferences were drawn by controlling the family-wise error (FWE) rate at a 0.05 threshold. Detailed descriptions of the DTI methods are available in the Supplementary material.

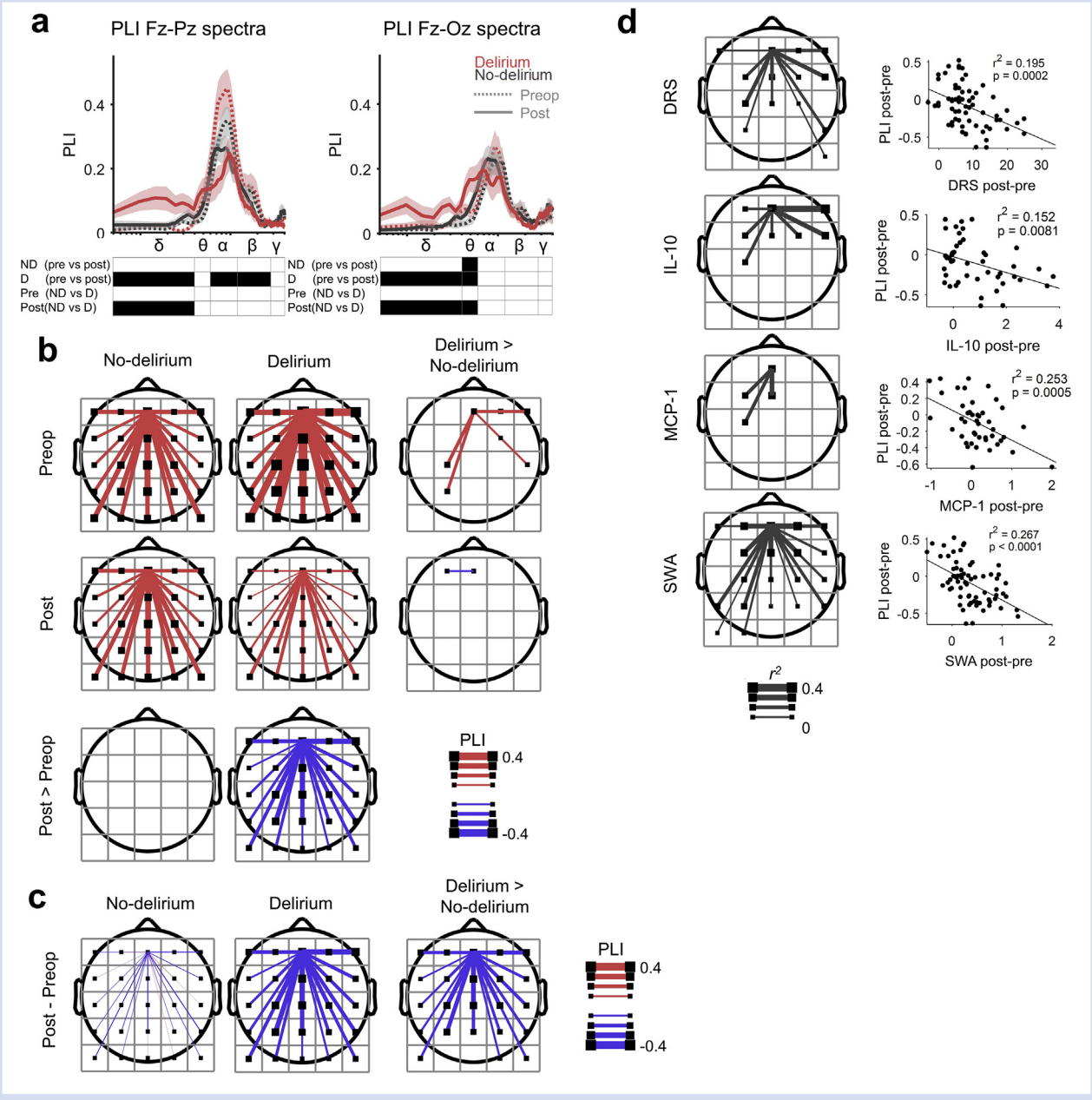

Fig 4. Delirium is associated with decreased connectivity (debiased weighted phase lag index [PLI]). (a) PLI spectral analysis comparing patients preoperatively (pre) and postoperatively (post) for patients who do (D), or do not (ND), incur delirium ($P<0.05$ [black squares]). Statistical analysis using a linear mixed-effects model across delirium states and pre-/postoperation is reported ($n_{ND}=48$ and $n_D=22$). Spectra range from 0.5 to 40 Hz; statistics done on frequency bands; δ 0.5–4 Hz, θ 4–6 Hz, α 6–12 Hz, β 12–28 Hz, and γ 28–40 Hz. (b) Topologically PLI of preoperative and postoperative states for patients who do not, or do, incur delirium. PLI with a frontal square group of electrodes is displayed and corrected. Bottom row shows postoperative>preoperative contrast ($P<0.05$ [line displayed if significant] after false discovery rate (FDR) correction with two-sided Wilcoxon signed-rank test). Right column shows contrast between patients who do, and do not, incur delirium, delirium>no delirium ($P<0.05$ after FDR correction with two-sided Wilcoxon rank-sum test; $n_{ND}=48$ and $n_D=22$). (c) Topological plots of the change in connectivity with transition to the non-delirious *vs* delirious state. Right, topoplot shows threshold-free cluster enhancement *t*-map of two groups contrast ($P<0.05$ after FDR correction with two-sided Wilcoxon rank-sum test; $n_{ND}=48$ and $n_D=22$). (d) Correlation of the postoperative–preoperative difference in PLI with changes in Delirium Rating of Severity-98 (DRS), interleukin (IL)-10, monocyte chemoattractant protein 1 (MCP-1), and slow-wave activity (SWA). Left column shows r^2 map ($P<0.05$ after FDR correction; DRS $n=70$ [64–69, after outlier exclusion], IL-10 $n=46$ [42–45], MCP-1 $n=47$ [42–46], and SWA $n=70$ [63–68]). Right columns show correlations with PLI of frontal square connecting to square below.

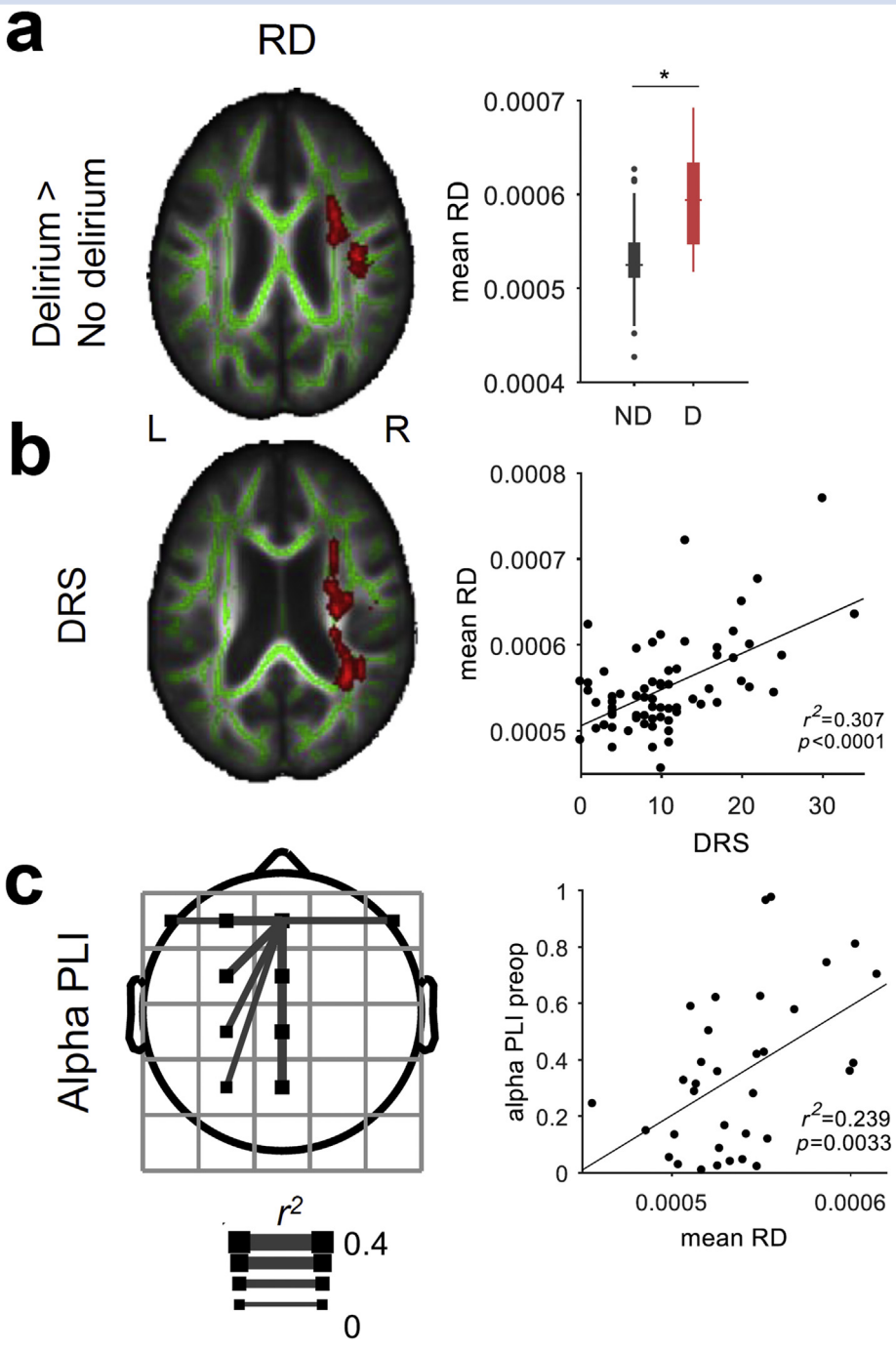

Fig 5. Preoperative connectivity is increased before delirium and inversely correlates with structural connectivity. (a) Preoperative radial diffusivity (RD) contrast for patients who do not incur delirium (ND) and do incur delirium (D) (general linear model with covariate age+gender; P<0.05 family-wise error corrected; n_{ND}=51 and n_D=17). Significant effects of RD (red) are overlaid on whole brain white matter tract (green). The right box plot shows mean RD contrast across significant voxels detected with multiple comparison correction between the groups (P<0.05 corrected; two-sided Wilcoxon rank-sum test). (b) Correlation of preoperative RD with peak postoperative delirium severity (general linear model with covariate age+gender; P<0.05 FWE corrected; n=68). (c) Correlation of preoperative (preop) topological alpha phase lag index (PLI) and mean RD across significant voxels (P<0.05 after false discovery rate correction; n=36 [33–36 after outlier exclusion]). Left, topoplot shows r^2 map for the PLI of frontal square is displayed and corrected. Right plot shows mean RD correlation with PLI of frontal square connecting to parietal square. DRS, Delirium Rating of Severity-98.

Results

Figure 1 shows the Strengthening the Reporting of Observational Studies in Epidemiology (STROBE) diagram and data collection strategy. Cohort characteristics are described in Supplementary Table 2. The median postoperative DRS was 9. Postoperative delirium occurred in 31% of patients, whose median DRS was 17. Delirious patients had similar age and sex to patients who did not become delirious, but they underwent operations with higher surgical severity (Wilcoxon rank-sum test; $P<0.001$; Supplementary Table 2).

EEG power spectral analyses

Initially, we focused on the within-subject change in the EEG that occurs from preoperative to postoperative phases of care. This showed obvious slowing on transition to the delirious state (Fig. 2a). For quantitative analysis, the EEG was initially segmented into different power bands, delta (0.5–4 Hz), theta (4–6 Hz), alpha (6–12 Hz), beta (12–28 Hz), and gamma (28–40 Hz), based on our division of data around the alpha peak that is evident in Fig. 2b. Our data show an increase in delta and theta power in frontal regions in both the non-delirious (linear mixed-effects model across delirium states and pre-/post-operation $P_{delta}<0.0001$ and $P_{theta}<0.0001$; Fig. 2c) and delirious ($P_{delta}<0.0001$ and $P_{theta}<0.0001$; Fig. 2d) subjects. A critical difference between patient groups was that delta and theta power increased in posterior regions in delirium, with a reciprocal decrease in higher-frequency activity (Fig. 2b and d). Interestingly, patients who later incurred delirium had higher frontal alpha power preoperatively ($P=0.0338$; Fig. 2b), but no change postoperatively. In contrast, frontal alpha power increased postoperatively in patients who did not incur delirium (Fig. 2c).

The preoperative differences between the subjects who did not incur delirium postoperatively and those that did emphasised the need to focus on the differences in EEG dynamics that occur on transition to delirium. Hence, we next confirmed that the *changes* in SWA that occur on transition from preoperative to postoperative state differed between the groups (described in Supplementary Fig. 2). This analysis was conducted to exclude non-specific EEG changes that may occur postoperatively (such as small increases in frontal SWA). In this focused analysis, increased global delta and theta power and loss of posterior high-frequency activity appeared characteristic of delirium (Fig. 2e and f).

Comparison of eyes-open and eyes-closed power spectra

The global increase in delta and theta power in delirious patients was surprising given that the subjects were sufficiently wakeful to complete our cognitive assessments. To confirm that the subjects were wakeful, we compared the power spectra for delirious subjects recorded with eyes open and closed (the latter being the typical state during the recordings). Whilst only three delirious patients were captured with eyes open (as delirious patients struggle to follow commands), there was no difference in the power spectra between the eyes-open and eyes-closed states, suggesting we were not merely studying sleep (Supplementary Fig. 3).

EEG power spectra sensitivity analyses

We next confirmed that this effect was not driven by patients requiring sedation for intubation on the ICU by performing a sensitivity analysis, excluding these seven patients (Supplementary Fig. 4). The results were unaffected by excluding these seven patients. As delta and theta bands showed similar effects across all these contrasts, henceforth we treated them as one frequency range, SWA, as has been done in studies of sleep deprivation.[19,29]

Correlations of EEG power and delirium severity

Next, we hypothesised that, as SWA increased, delirium severity would worsen. We calculated the Pearson correlation of power, for each frequency band, with the change in delirium severity (DRS). For the purpose of display, we also show the correlation coefficient in 0.1 Hz frequency bins. Slow-wave activity showed a remarkable correlation with DRS with specificity at <6 Hz, such that, as SWA increased, delirium severity increased (Fig. 3a). Topographic analysis showed that, whilst there were significant correlations of DRS and SWA in many electrodes across the scalp, the relationship appeared strongest in posterior regions. Indeed, at electrode Oz, the correlation was relatively strong ($r^2=0.207$; $P=0.0001$). However, there was no statistical difference between Fz and Oz for the correlation with DRS with a Williams test; $P=0.67$. We identified a similar effect when excluding the seven patients on sedation (Supplementary Fig. 4), and confirmed that all delirious subjects showed increases in Oz SWA (Supplementary Fig. 5). Correlations of DRS with EEG changes in higher frequencies were not observed, suggesting these changes may not be causally related to the delirium state (Supplementary Fig. 6). These data suggest that SWA is a key feature of delirium.

Correlations of EEG power and cytokines

We looked for associations between cytokine changes and delirium using a multiplex panel of 10 cytokines (Eve Technologies) using Bonferroni multiple comparison correction. Consistent with prior studies,[30] we identified significant associations of simultaneous changes in MCP-1 ($r^2=0.192$; $P=0.002$) and IL-10 ($r^2=0.200$; $P=0.002$), with both delirium severity (DRS; Supplementary Fig. 7) *and* delirium incidence (Supplementary Fig. 8). The other cytokines did not achieve significance on both tests. Given the detected and plausible association with delirium, we tested whether MCP-1 and IL-10 were also correlated with SWA. Similar <6 Hz changes in posterior electrode SWA were correlated with these two cytokines (Fig. 3c and d), suggesting that systemic inflammation may drive SWA.

EEG connectivity analyses

To address whether integration also fades in delirium, we measured functional connectivity using PLI.[20] We hypothesised that, whilst local SWA in frontal cortex was insufficient to cause delirium, when SWA transitioned to be global, the ensuing reduction in cortical connectivity precipitated delirium. First, we confirmed that alpha band was the appropriate frequency range to explore in our data (as suggested by a prior study[11]) by plotting the PLI spectrum in 0.4883 Hz frequency resolution. Indeed, there was a clear peak in connectivity in the alpha range preoperatively (linear mixed-effects model across delirium states and pre-/postoperation $P_{alpha}<0.0001$; Fig. 4a). Delirium was also associated with an increase in Fz-Pz connectivity in the delta range (Fig. 4a).

To make our analysis sensitive to change in the non-delirious group (where we observed increases in SWA post-operatively), we placed a connectivity seed in frontal regions (see Supplementary Fig. 1 for methodological description) and calculated connectivity with other scalp regions. In case-control analyses (Fig. 4b rows), preoperatively, patients who subsequently became delirious showed increased frontal connectivity. Postoperatively, however, they showed decreased connectivity.

Change in connectivity from preoperative levels

We next analysed the *change in connectivity* from preoperative to postoperative state across groups. In the non-delirious subjects, there was no change in connectivity from the preoperative period, consistent with only localised SWA (Fig. 4b, columns). However, the transition into delirium was associated with significant decreases in frontal connectivity with posterior brain regions (Fig. 4c). Of delirious subjects, 19 showed decreases in Fz-Pz alpha PLI and three showed increases (Supplementary Fig. 9).

Connectivity sensitivity analyses

The results without outlier rejection are presented in Supplementary Fig. 10. We confirmed changes of connectivity that correlated with DRS with calculations of pairwise connectivity between all electrodes and a conservative FDR correction across pairwise connections (Supplementary Fig. 11). These data emphasised the correlations of fronto-temporal connections with delirium severity. In sum, our data suggest that, in delirium, as SWA extends to reach posterior brain regions, there is an associated breakdown in brain connectivity.

Possible mechanistic associations of the change in connectivity

Changes in connectivity were also correlated with SWA (r^2=0.257; P<0.0001), DRS (r^2=0.195; P<0.001), IL-10 (r^2=0.152; P=0.008), and MCP-1 (r^2=0.253; P<0.001; Fig. 4d).

Post hoc investigation into preoperative structural connectivity and delirium

One aspect of these connectivity observations is particularly at odds with our published hypothesis of delirium.[7] Preoperatively, subjects who would later become delirious had higher EEG functional connectivity than subjects who did not become delirious. *Prima facie*, this observation also seemed to contradict extensive prior data showing impaired structural connectivity before delirium; see for example Cavallari and colleagues.[27] Therefore, we analysed available structural connectivity using preoperative DTI. Consistent with prior data,[27] preoperatively, patients before delirium had impaired structural connectivity, reflected by increased RD, adjusted for age and gender as detected using TBSS in FSL (voxel-wise statistics: number of voxels=4260, FWE P=0.047, t=4.5; mean statistics: $RD_{delirium}$>$RD_{non\text{-}delirium}$ with Wilcoxon rank-sum test; P<0.001; Fig. 5a; Supplementary Table 3). Again, similar to prior results,[27] increased preoperative RD values also correlated with increasing postoperative delirium severity, adjusted for age and gender (voxel-wise statistics: number of voxels=5595, FWE P=0.044, t=5.23; mean statistics: association of mean RD in significant voxels and delirium severity was r^2=0.29, P<0.001; Fig. 5b). Similar findings were observed in MD as well, when adjusted for age and gender (*delirium incidence*: voxel-wise statistics: number of voxels=4757, FWE P=0.026, t=5.33; mean statistics: mean statistics: $MD_{delirium}$>$MD_{non\text{-}delirium}$ with Wilcoxon rank-sum test, P<0.001; *delirium severity*: voxel-wise statistics: number of voxels=3747, FWE P=0.036, t=4.41; mean statistics: association of mean MD in significant voxels and delirium severity was r^2=0.2, P<0.001; Supplementary Fig. 12; Supplementary Table 4). Associations with AD and FA were not identified (data not shown).

Post hoc investigation into preoperative structural connectivity and EEG functional connectivity

We hypothesised that increased functional connectivity in the EEG may represent a mechanism of compensation for underlying structural pathology based on recent hypotheses from neuroimaging.[31] Next, we quantified the mean value of RD across voxels that correlated with delirium severity, and looked for how these correlated with the preoperative EEG connectivity measures. To do this, we correlated the measure with topographic EEG connectivity, testing whether the functional connectivity changes in the EEG reflected a compensatory response to the underlying structural pathology. Positive correlations were noted, focused on left frontal regions, for the relationship of RD and alpha band frontal connectivity (electrode Fz r^2=0.491; P=0.0012; Fig. 5c). These data suggest that, as structural connectivity worsened (higher RD) on the right, functional connectivity of the EEG increased on the left, supporting the concept that increased preoperative functional connectivity is a compensatory mechanism for underlying structural neurodegeneration.

Discussion

Our data suggest that local frontal SWA can occur post-operatively, but does not result in delirium. Rather, post-operative delirium results when inflammation-driven SWA extends to involve occipitoparietal cortex associated with a breakdown in connectivity. Our prior hypothesis[7] emphasised the role of connectivity in delirium; a subsequent study supported this idea,[11] but did not relate the changes mechanistically to SWA, inflammation, or investigate proportionality to delirium severity. That study was also limited by its case-control design. We have shown clear links to inflammatory models of delirium through correlation of contemporaneous changes in systemic cytokines, and relate the connectivity changes to SWA. Whilst we are presently unable to manipulate delirium experimentally to test causal mechanisms, our data are strongly supported by several Bradford Hill criteria for causality: *temporal sequence*, *strength* of change, and *dose dependence*. Our data also show *coherence* with the dementia literature[32–36] and *biological plausibility* based on both the links between inflammation and delirium,[37] and also the changes in SWA following sleep deprivation and consequent impairments in cognition.[19,29]

An unexpected finding was that of increased frontal high-frequency power and alpha band connectivity before delirium. We speculate that these changes were compensatory responses to underlying neurodegeneration, and provided evidence for this from structural imaging data. Increased frontal alpha power has recently been identified as a signature of amyloid disease.[38] As an extension of recent hypotheses

from neuroimaging,[31] we surmise that these electrophysiological changes may represent evidence of functional compensations whereby increased network connectivity is recruited as a mechanism to maintain cognitive function from chronic neurodegenerative pathologies. Interestingly, the non-delirious subjects showed an increase in frontal alpha power and maintained cognitive function postoperatively. Increased alpha activity and connectivity may be a key compensatory mechanism to maintain cognitive function in the presence of a physiological stressor (such as inflammation). Increasing 8 Hz frontotemporal connectivity (within our alpha range) has recently been shown to improve cognitive performance in the older population.[39] We have replicated and extended prior work[10,11] showing that decreases in alpha band connectivity may contribute to the cognitive dysfunction in delirium, although it is important to note that decreases in alpha band connectivity did not occur in all delirious subjects. It is presently unclear whether these subjects showed connectivity changes in other bands leading to delirium, or whether connectivity changes do not contribute to delirium in these subjects. Nonetheless, manipulation of alpha band connectivity may yet prove to be a therapy for delirium in at least some subjects.

We note some important limitations of our study. Firstly, the cohort was of modest size, and it may be that more diverse changes may be identified in a larger cohort, or alternative changes may occur in other types of delirium, for example, those induced by medications. We acknowledge these limitations, but stress that we have likely identified the strongest relationships, which are most likely to be causal, and that inflammation is a very common mechanism of delirium[6] (as delirium by definition arises from a physiological stressor). Nonetheless, our focus on inflammation does not imply that the associations we have discovered will extend to other clinical settings or mechanistic types of delirium, where pathologies other than inflammation may play a larger role. Secondly, it is not possible to perform more invasive electrophysiological studies in most types of delirium. Thirdly, it is possible that some form of unmeasured confounding may still affect our results; however, we control for the baseline state and calculated changes in the perioperative period. This approach, essentially normalising to the baseline state, adjusts for many of the confounds of the baseline state, including age and co-morbidities. This is critical, given we have observed preoperative differences in the EEG. We also conducted sensitivity analyses for cohort type (IPOD-B2 *vs* IPOD-B3) and exposure to sedative medications.

In summary, our data show that changes in occipitoparietal cortical SWA correlated with worsening delirium severity, systemic inflammation, and impaired connectivity. Hence, whilst frontal, local SWA occurs in postoperative patients, delirium results when SWA progresses to involve posterior brain regions, with an associated reduction in connectivity.

Authors' contributions

Study design: RDS, MIB
Data collection/analysis: RDS, ST, HL, CC, ZF, TB, RM
Devising of imaging protocol: VP
Imaging analyses: RM, VP
EEG analyses: ST, RDS, MIB
Statistical advice: BK
Writing of paper: RDS, ST

Declaration of interest

The authors declare that they have no conflicts of interest.

Funding

National Institutes of Health (K23 AG055700) to RDS; National Institutes of Health (R01 AG063849-01) to RDS; National Heart, Lung, and Blood Institute (5T32HL091816-07) to HL.

Acknowledgements

The authors thank Drs Brady Riedner and Giulio Tononi for advice and loan of EEG equipment.

Appendix A. Supplementary data

Supplementary data to this article can be found online at https://doi.org/10.1016/j.bja.2020.02.027.

References

1. Inouye SK, Westendorp RG, Saczynski JS. Delirium in elderly people. *Lancet* 2014; **383**: 911–22
2. Witlox J, Eurelings LS, de Jonghe JF, Kalisvaart KJ, Eikelenboom P, van Gool WA. Delirium in elderly patients and the risk of postdischarge mortality, institutionalization, and dementia: a meta-analysis. *JAMA* 2010; **304**: 443–51
3. Leslie DL, Marcantonio ER, Zhang Y, Leo-Summers L, Inouye SK. One-year health care costs associated with delirium in the elderly population. *Arch Intern Med* 2008; **168**: 27–32
4. Hshieh TT, Fong TG, Marcantonio ER, Inouye SK. Cholinergic deficiency hypothesis in delirium: a synthesis of current evidence. *J Gerontol A Biol Sci Med Sci* 2008; **63**: 764–72
5. Cerejeira J, Firmino H, Vaz-Serra A, Mukaetova-Ladinska EB. The neuroinflammatory hypothesis of delirium. *Acta Neuropathol* 2010; **119**: 737–54
6. Cunningham C, Maclullich AM. At the extreme end of the psychoneuroimmunological spectrum: delirium as a maladaptive sickness behaviour response. *Brain Behav Immun* 2013; **28**: 1–13
7. Sanders RD. Hypothesis for the pathophysiology of delirium: role of baseline brain network connectivity and changes in inhibitory tone. *Med Hypotheses* 2011; **77**: 140–3
8. Tononi G. An information integration theory of consciousness. *BMC Neurosci* 2004; **5**: 42
9. Bastos AM, Usrey WM, Adams RA, Mangun GR, Fries P, Friston KJ. Canonical microcircuits for predictive coding. *Neuron* 2012; **76**: 695–711
10. Numan T, Slooter AJC, van der Kooi AW, et al. Functional connectivity and network analysis during hypoactive delirium and recovery from anesthesia. *Clin Neurophysiol* 2017; **128**: 914–24
11. van Dellen E, van der Kooi AW, Numan T, et al. Decreased functional connectivity and disturbed directionality of information flow in the electroencephalography of intensive care unit patients with delirium after cardiac surgery. *Anesthesiology* 2014; **121**: 328–35
12. Murphy M, Riedner BA, Huber R, Massimini M, Ferrarelli F, Tononi G. Source modeling sleep slow waves. *Proc Natl Acad Sci U S A* 2009; **106**: 1608–13
13. Murphy M, Bruno MA, Riedner BA, et al. Propofol anesthesia and sleep: a high-density EEG study. *Sleep* 2011; **34**: 283–91

14. Ponten SC, Tewarie P, Slooter AJ, Stam CJ, van Dellen E. Neural network modeling of EEG patterns in encephalopathy. *J Clin Neurophysiol* 2013; **30**: 545–52
15. Inouye SK, van Dyck CH, Alessi CA, Balkin S, Siegal AP, Horwitz RI. Clarifying confusion: the confusion assessment method. A new method for detection of delirium. *Ann Intern Med* 1990; **113**: 941–8
16. Marcantonio ER, Ngo LH, O'Connor M, et al. 3D-CAM: derivation and validation of a 3-minute diagnostic interview for CAM-defined delirium: a cross-sectional diagnostic test study. *Ann Intern Med* 2014; **161**: 554–61
17. Ely EW, Inouye SK, Bernard GR, et al. Delirium in mechanically ventilated patients: validity and reliability of the confusion assessment method for the intensive care unit (CAM-ICU). *JAMA* 2001; **286**: 2703–10
18. Trzepacz PT, Mittal D, Torres R, Kanary K, Norton J, Jimerson N. Validation of the Delirium Rating Scale-revised-98: comparison with the delirium rating scale and the cognitive test for delirium. *J Neuropsychiatry Clin Neurosci* 2001; **13**: 229–42
19. Nir Y, Andrillon T, Marmelshtein A, et al. Selective neuronal lapses precede human cognitive lapses following sleep deprivation. *Nat Med* 2017; **23**: 1474–80
20. Vinck M, Oostenveld R, van Wingerden M, Battaglia F, Pennartz CM. An improved index of phase-synchronization for electrophysiological data in the presence of volume-conduction, noise and sample-size bias. *Neuroimage* 2011; **55**: 1548–65
21. Smith SM, Nichols TE. Threshold-free cluster enhancement: addressing problems of smoothing, threshold dependence and localisation in cluster inference. *Neuroimage* 2009; **44**: 83–98
22. Neter J, Kutner MH, Nachtsheim CJ, Wasserman W. *Applied linear statistical models*. Chicago, IL: McGraw-Hill; 1996
23. Andersson JLR, Sotiropoulos SN. An integrated approach to correction for off-resonance effects and subject movement in diffusion MR imaging. *Neuroimage* 2016; **125**: 1063–78
24. Smith SM, Jenkinson M, Woolrich MW, et al. Advances in functional and structural MR image analysis and implementation as FSL. *Neuroimage* 2004; **23**: S208–19
25. Avants BB, Tustison NJ, Song G, Cook PA, Klein A, Gee JC. A reproducible evaluation of ANTs similarity metric performance in brain image registration. *Neuroimage* 2011; **54**: 2033–44
26. Schwarz CG, Gunter JL, Ward CP, et al. The Mayo clinic adult life span template: better quantification across the life span. *Alzheimers Dement* 2017; **13**: P93–4
27. Cavallari M, Dai W, Guttmann CR, et al. Neural substrates of vulnerability to postsurgical delirium as revealed by presurgical diffusion MRI. *Brain* 2016; **139**: 1282–94
28. Smith SM, Jenkinson M, Johansen-Berg H, et al. Tract-based spatial statistics: voxelwise analysis of multi-subject diffusion data. *Neuroimage* 2006; **31**: 1487–505
29. Vyazovskiy VV, Olcese U, Hanlon EC, Nir Y, Cirelli C, Tononi G. Local sleep in awake rats. *Nature* 2011; **472**: 443–7
30. van den Boogaard M, Kox M, Quinn KL, et al. Biomarkers associated with delirium in critically ill patients and their relation with long-term subjective cognitive dysfunction; indications for different pathways governing delirium in inflamed and noninflamed patients. *Crit Care* 2011; **15**: R297
31. Sala-Llonch R, Bartres-Faz D, Junque C. Reorganization of brain networks in aging: a review of functional connectivity studies. *Front Psychol* 2015; **6**: 663
32. Babiloni C, Binetti G, Cassetta E, et al. Sources of cortical rhythms change as a function of cognitive impairment in pathological aging: a multicenter study. *Clin Neurophysiol* 2006; **117**: 252–68
33. Babiloni C, Del Percio C, Lizio R, et al. Abnormalities of resting state cortical EEG rhythms in subjects with mild cognitive impairment due to Alzheimer's and Lewy body diseases. *J Alzheimers Dis* 2018; **62**: 247–68
34. Gianotti LR, Kunig G, Lehmann D, et al. Correlation between disease severity and brain electric LORETA tomography in Alzheimer's disease. *Clin Neurophysiol* 2007; **118**: 186–96
35. Stam CJ, de Haan W, Daffertshofer A, et al. Graph theoretical analysis of magnetoencephalographic functional connectivity in Alzheimer's disease. *Brain* 2009; **132**: 213–24
36. Engels MM, Stam CJ, van der Flier WM, Scheltens P, de Waal H, van Straaten EC. Declining functional connectivity and changing hub locations in Alzheimer's disease: an EEG study. *BMC Neurol* 2015; **15**: 145
37. Cape E, Hall RJ, van Munster BC, et al. Cerebrospinal fluid markers of neuroinflammation in delirium: a role for interleukin-1beta in delirium after hip fracture. *J Psychosom Res* 2014; **77**: 219–25
38. Nakamura A, Cuesta P, Fernandez A, et al. Electromagnetic signatures of the preclinical and prodromal stages of Alzheimer's disease. *Brain* 2018; **141**: 1470–85
39. Reinhart RMG, Nguyen JA. Working memory revived in older adults by synchronizing rhythmic brain circuits. *Nat Neurosci* 2019; **22**: 820–7

Handling editor: Michael Avidan